Cell PRESS
Neuron
Report

TRPC3 Channels Are Required for Synaptic Transmission and Motor Coordination

Jana Hartmann,[1] Elena Dragicevic,[1] Helmuth Adelsberger,[1] Horst A. Henning,[1] Martin Sumser,[1] Joel Abramowitz,[2] Robert Blum,[3] Alexander Dietrich,[4] Marc Freichel,[5] Veit Flockerzi,[5] Lutz Birnbaumer,[2] and Arthur Konnerth[1,*]
[1]Institute of Neuroscience and Center for Integrated Protein Science, Technical University Munich, 80802 Munich, Germany
[2]Transmembrane Signaling Group, National Institute of Environmental Health Sciences, Research Triangle Park, NC 27709, USA
[3]Institute of Physiology, Ludwig-Maximilians-University Munich, 80336 Munich, Germany
[4]Institute of Pharmacology and Toxicology, Philipps-University Marburg, 35043 Marburg, Germany
[5]Institute of Experimental and Clinical Pharmacology and Toxicology, Saarland University, 66421 Homburg (Saar), Germany
*Correspondence: arthur.konnerth@lrz.tum.de
DOI 10.1016/j.neuron.2008.06.009

SUMMARY

In the mammalian central nervous system, slow synaptic excitation involves the activation of metabotropic glutamate receptors (mGluRs). It has been proposed that C1-type transient receptor potential (TRPC1) channels underlie this synaptic excitation, but our analysis of TRPC1-deficient mice does not support this hypothesis. Here, we show unambiguously that it is TRPC3 that is needed for mGluR-dependent synaptic signaling in mouse cerebellar Purkinje cells. TRPC3 is the most abundantly expressed TRPC subunit in Purkinje cells. In mutant mice lacking TRPC3, both slow synaptic potentials and mGluR-mediated inward currents are completely absent, while the synaptically mediated Ca^{2+} release signals from intracellular stores are unchanged. Importantly, TRPC3 knockout mice exhibit an impaired walking behavior. Taken together, our results establish TRPC3 as a new type of postsynaptic channel that mediates mGluR-dependent synaptic transmission in cerebellar Purkinje cells and is crucial for motor coordination.

INTRODUCTION

Group I metabotropic glutamate receptors of subtype 1 (mGluR1) are G protein-coupled receptors (Sugiyama et al., 1987) that are abundantly expressed in the cerebellum (Martin et al., 1992). They have an essential role for normal motor behavior in mammals. Their absence in knockout mice causes a pronounced ataxia (Aiba et al., 1994) that can be rescued by the selective expression of mGluR1 in cerebellar Purkinje neurons (Ichise et al., 2000). In Purkinje neurons, activation of mGluR1 mediates a synaptic response consisting of two components, namely a slow excitatory postsynaptic potential (EPSP) (Batchelor and Garthwaite, 1993) and a Ca^{2+} release signal from intracellular stores (Finch and Augustine, 1998; Takechi et al., 1998). The mechanisms underlying synaptically evoked Ca^{2+} release from stores are well established. Thus, at parallel fiber (PF) synapses, repetitive afferent stimulation leads to the activation of mGluR1 followed by the activation of a signaling cascade consisting of $G\alpha_q$ and $G\alpha_{11}$ (Hartmann et al., 2004), phospholipase Cβ (PLC-β), and eventually inositol-1,4,5-trisphosphate ($InsP_3$) (Finch and Augustine, 1998; Hirono et al., 1998; Takechi et al., 1998). By contrast, the mechanisms underlying the slow EPSP are less clear. Over the last several years, accumulating evidence indicated an involvement of a TRP-type (Ramsey et al., 2006; Venkatachalam and Montell, 2007) nonselective cation channel (Canepari et al., 2001; Hirono et al., 1998; Tempia et al., 2001). In a relatively recent report, Kim et al. (2003) proposed, based on manipulations that interfere with TRPC1 function, that TRPC1 cation channels underlie the slow EPSP. While these experiments provided compelling evidence for a role of TRPC1 in vitro, many questions remained open. These include the role of other TRPC cation channels and, importantly, the relevance of TRPC channels for physiological functions in vivo. Therefore, we set out to analyze mice lacking distinct TRPC channel subtypes.

RESULTS

We examined synaptic transmission at PF-Purkinje neuron synapses in acute mouse cerebellar slices by combining whole-cell voltage-clamp recordings and confocal calcium imaging. Afferent PFs were activated by a stimulation pipette that was placed on the slice surface above the dendrites under investigation (Figure 1A). As previously reported (Hartmann et al., 2004; Takechi et al., 1998), burst-like repetitive stimulation produces a rapid inward current that is mainly mediated by AMPA receptors and a slow component mediated by mGluR1 (Figure 1C, control, bottom). For a better separation of the two components, these recordings were performed in the presence of the AMPA receptor antagonist 6-cyano-7-nitroquinoxaline-2,3-dione (CNQX; 10 μM), which reduced the amplitude of the rapid EPSC by about 90% (Kim et al., 2003). In addition to the compound electrical response, synaptic stimulation evoked a large Ca^{2+} transient (Figure 1C, control, top) that was confined to a restricted dendritic area near the site of synaptic stimulation (Takechi et al., 1998) (Figure 1B). Application of the mGluR1 antagonist CPCCOEt (200 μM) selectively abolished the slow EPSC and the Ca^{2+} transient (Figure 1C, red traces). Under our conditions

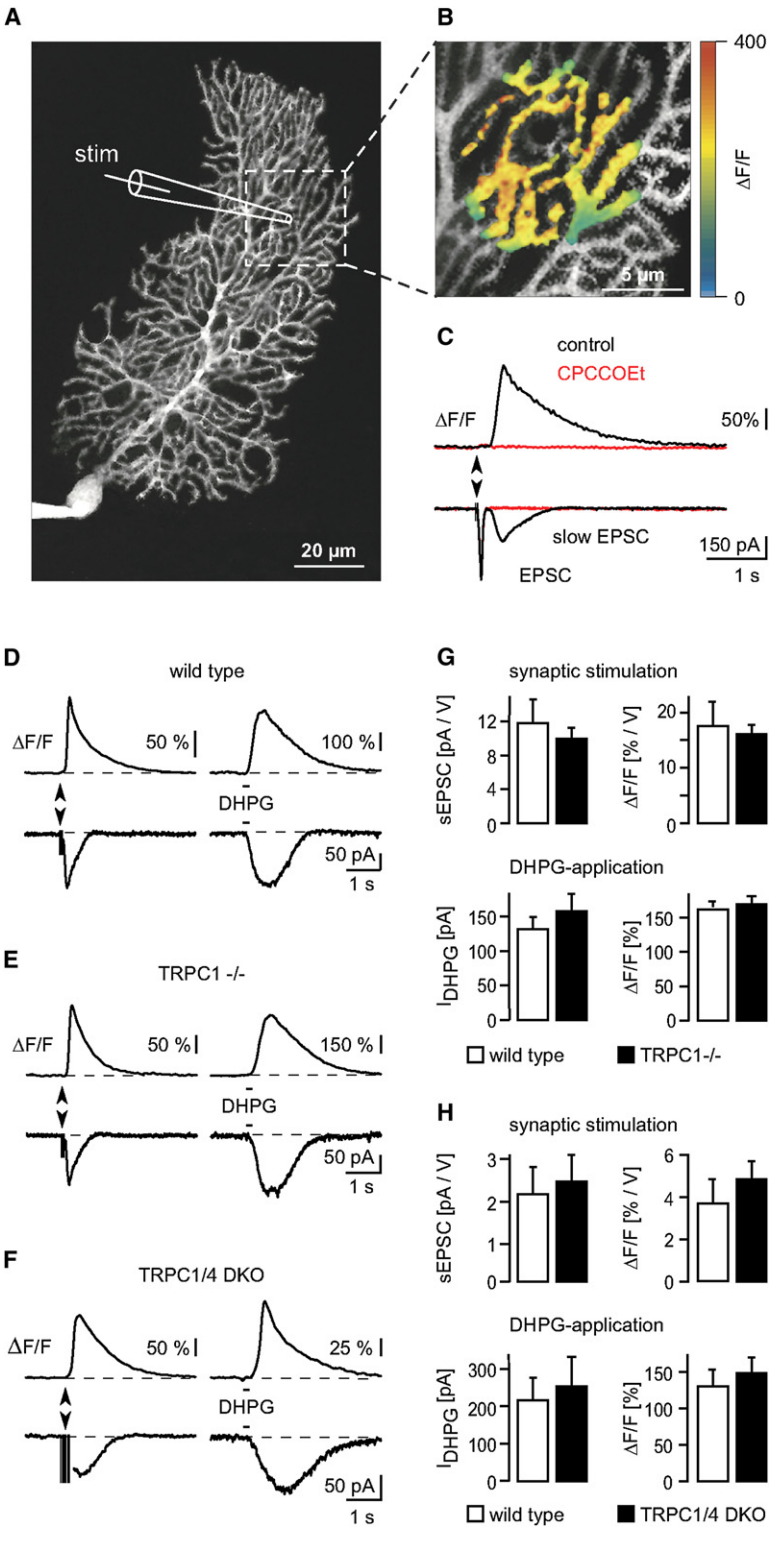

Figure 1. mGluR-Mediated Purkinje Cell Signaling in the Absence of TRPC1 and TRPC4 Subunits

(A) Confocal image of a patch-clamped Purkinje cell in a cerebellar slice from a wild-type (WT) mouse. The site of electrical stimulation (stim) is shown at higher magnification in (B). (B) Pseudocolor image of a synaptic Ca^{2+} signal evoked by parallel fiber (PF) stimulation. (C) Black traces: PF-evoked (five pulses, 100 Hz, in 10 μM CNQX) synaptic response consisting of an early rapid and a slow EPSC (bottom) and a Ca^{2+} transient (top). Red traces: Block of slow components by CPCCOEt (200 μM). (D) (Left) Slow EPSC (ten pulses, 100 Hz in 40 μM CNQX) in a WT mouse (lower trace) and the corresponding local Ca^{2+} response (upper trace). (Right) Pressure ejection of DHPG (200 μM for 100 ms) evoked a slow inward current (lower trace) and a local Ca^{2+} transient (upper trace). Similar experiments performed in TRPC1-knockout (E) and in TRPC1/TRPC4 DKO mice (F) using PF stimulation (left panels; 15 pulses, 50 Hz) and local DHPG pressure application (right panels; 1 mM, 100 ms), respectively. (G and H) Summary of the results obtained in WT and *TRPC1*$^{-/-}$ mice (mean ± SEM; [G]: n = 16 and n = 22 for synaptic transmission, n = 38 and n = 30 for DHPG applications in WT and *TRPC1*$^{-/-}$, respectively) and in TRPC1/4 DKO mice ([H]: n = 12 and n = 21 for synaptic transmission, n = 13 and n = 8 for DHPG applications in WT and TRPC1/4 DKO, respectively). Responses in mutants were not significantly different from those in WT (Student's t test).

of voltage-clamp recordings and reduced AMPA receptor activation, the Ca^{2+} transient was almost completely mediated by mGluR1, without a significant contribution of Ca^{2+} entry through voltage-gated Ca^{2+} channels (Eilers et al., 1995).

Figures 1D–1F show recordings in which we focused exclusively on mGluR1-mediated signaling by performing experiments in the presence of CNQX at a concentration that blocked the rapid EPSC completely (40 μM). Under these conditions, repetitive synaptic stimulation (ten pulses, 100 Hz) evoked in wild-type (WT) mice a slow EPSC and the corresponding Ca^{2+} transient (Figure 1D, left; n = 16). It is important to stress that this synaptically evoked Ca^{2+} transient is predominantly the result of $InsP_3$-mediated Ca^{2+} release from internal stores (Canepari and Ogden, 2006; Takechi et al., 1998). Figure 1D (right) shows that application of the mGluR1 agonist DHPG, locally to the dendrites, also produced an inward current and a local dendritic Ca^{2+} transient (n = 38). Figure 1E demonstrates that, to our surprise, TRPC1-deficient mice (Dietrich et al., 2007) had a normal mGluR1-mediated synaptic transmission and normal DHPG-evoked signaling, with no obvious impairment of the slow EPSC or the Ca^{2+} transient. Similar results were obtained in all our experiments (n = 22 for synaptic transmission; n = 30 for DHPG applications). Next, we analyzed newly generated TRPC1-TRPC4 double-knockout mice (TRPC1/4 DKO) and TRPC1-TRPC4-TRPC6 triple-knockout mice (TRPC1/4/6 TKO) (Dietrich et al., 2005; Freichel et al., 2001; see also Supplemental Data available online) using 15 pulses at 50 Hz for PF stimulation. In both types of mouse mutants, TRPC1/4 DKO (Figure 1F) and TRPC1/4/6 TKO (Figure S1), we detected normal mGluR1-mediated

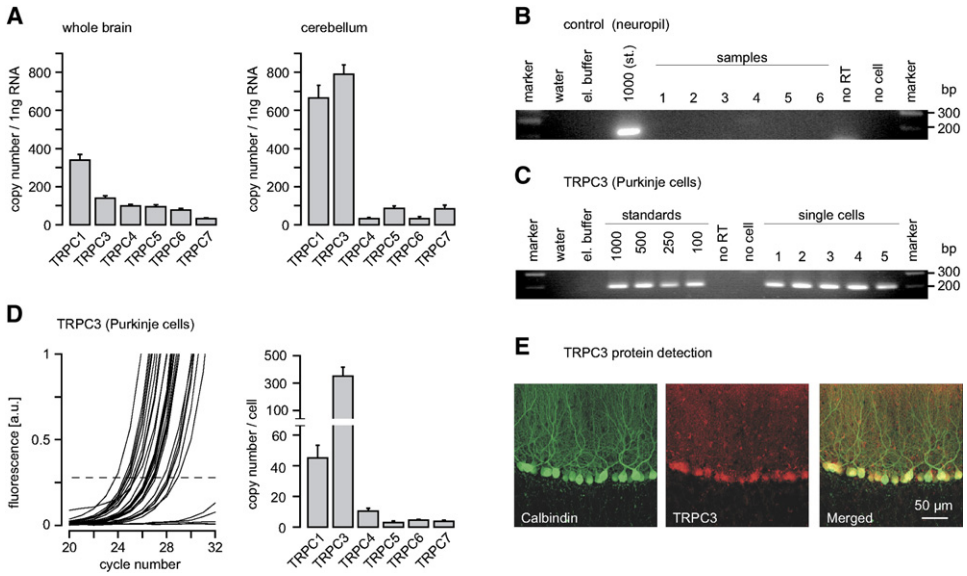

Figure 2. Expression Pattern of TRPC Channel Subunits in the Mouse Brain and Single Purkinje Cells

(A) Copy numbers of TRPC subunit mRNA detected in 1 ng total RNA of mouse whole brain (left) and cerebellum (right; mean ± SEM).

(B) Agarose gel electrophoresis of the TRPC1 amplicons in the neuropil material surrounding Purkinje cell somata. The gene-specific standard (1000 copies) was used as a positive control.

(C) Analogous agarose gel electrophoresis of *TRPC3* amplicons obtained from single Purkinje cells.

(D) (Left) Real-time monitoring of the fluorescence emission of SYBR Green I during the PCR amplification of *TRPC3* cDNA from single Purkinje cells (n = 34 cells). (Right) Copy numbers of transcripts of TRPC subunits in single Purkinje cells (mean ± SEM).

(E) A dual-channel confocal scan of an immunohistochemical staining in an acute cerebellar slice. Calbindin-D_{28k} immunoreactivity is shown in green (left) and that for TRPC3 is shown in red (middle). (Right) merged images.

synaptic transmission. Figures 1G and 1H summarize the results for TRPC1-deficient and TRPC1/4 DKO mice compared to the corresponding WT mice, respectively. In both *TRPC1*$^{-/-}$ and in TRPC1/4 DKO mice, mGluR-mediated responses were not significantly different from those recorded in WT mice. Furthermore, normal mGluR-mediated responses were also observed in TRPC1/4/6 TKO mice following synaptic stimulation or DHPG-application (Figure S1). Importantly, *TRPC1*$^{-/-}$ (Figure S3) as well as TRPC1/4 DKO and TRPC1/4/6 TKO mice showed no signs of abnormal motor behavior. Taken together, these results demonstrate that neither TRPC1 nor TRPC4 nor TRPC6 are essential for the mGluR-mediated slow EPSC.

The absence of any major role of TRPC1, TRPC4, or TRPC6 for mGluR-mediated signaling fits to the observation that the expression level of these receptors is quite low in Purkinje cells. Instead, there is evidence for a prominent expression of TRPC3 in cerebellar Purkinje cells (Huang et al., 2007; see also Allen Brain Atlas at http://brain-map.org). For a more accurate assessment of the expression level of TRPC channels in brain, cerebellum, and Purkinje cells, we used a quantitative rapid-cycle RT-PCR approach (Durand et al., 2006; Hartmann et al., 2004). Figure 2A (left) shows data indicating that in the whole brain the most abundantly expressed TRPC subunit is TRPC1 (Riccio et al., 2002). By contrast, in the cerebellum (Figure 2A, right), TRPC3 is slightly more abundant than TRPC1, while the remaining TRPC channels are expressed at low levels.

For the analysis of single Purkinje cells, we used a procedure involving the harvesting of individual cells from acute cerebellar slices by means of a fine suction pipette (Durand et al., 2006). With this procedure, we reliably detected transcripts for *TRPC3* (Figures 2C and 2D) as well as transcripts for *TRPC1*, *TRPC4*, *TRPC5*, *TRPC6*, and *TRPC7*. The analysis of the TRPC2 subunit, which is known to be virtually absent in the brain (Huang et al., 2007; Liman et al., 1999), was not included in this study. Figure 2B illustrates one of our routinely performed control experiments showing the absence of TRPC1, the expected most abundant TRPC channel outside Purkinje cells, in neuropil tissue samples collected near the Purkinje cell layer. Figure 2D (right) shows the results obtained in individual Purkinje cells. These findings indicate that, at least in terms of mRNA, TRPC3 is by far the most abundantly expressed TRPC channel in Purkinje cells. TRPC3 mRNA is eight to ten times more abundant than TRPC1 mRNA, while the amount of mRNA coding for the other TRPC channels is almost negligible. Figure 2E confirms at the protein level the presence of TRPC3 subunits in Purkinje cells (Huang et al., 2007).

In view of these results, we generated a mutant mouse that lacks TRPC3. We used a *Cre-loxP*-based strategy in order to excise exon 7 from the *TRPC3* gene (see Experimental Procedures and Figure S1). Figure 3A (upper scheme) depicts the result of the first step in this procedure, namely the inclusion of *loxP* sequences on both sides of exon 7. For the insertion of the Cre recombinase, a mouse line that expresses Cre under the control of a promotor with ubiquitous activity in the early embryo (Mox2; Tallquist and Soriano, 2000) was used. The result of recombination is a general deletion of exon 7 from the *TRPC3* gene, shown

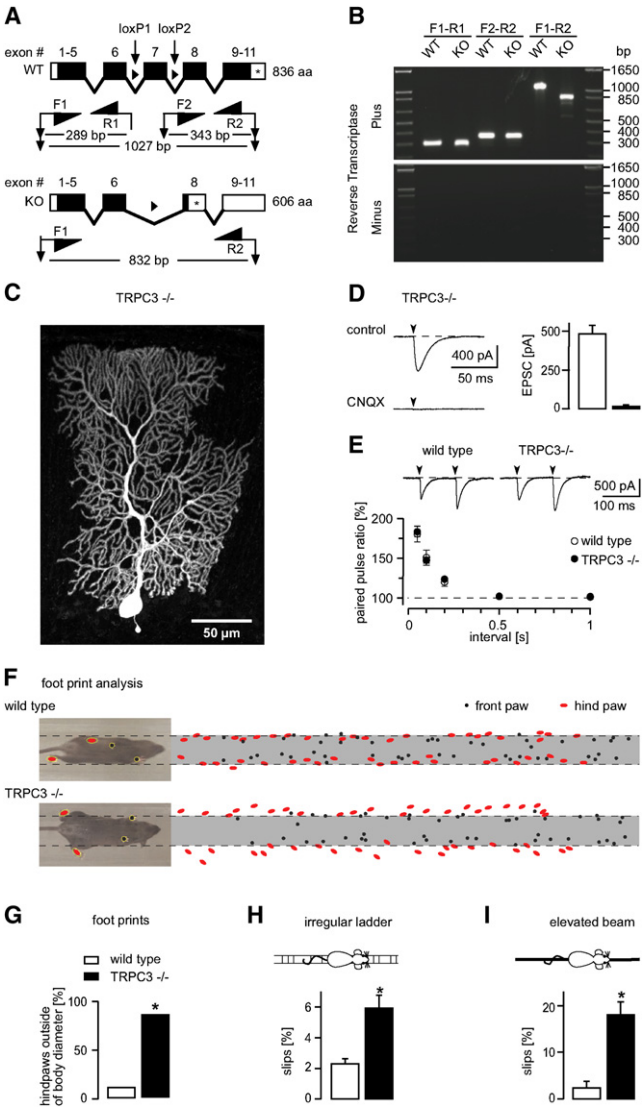

Figure 3. Generation and Characterization of a TRPC3 Knockout Mouse

(A) (Top) Diagram of the intron-exon organization of the *Mus musculus TRPC3* gene. Open boxes, untranslated exonic sequence; closed boxes, translated open reading frame; *, stop codon; F1, F2, R1, and R2: PCR primers. The lengths of the amplicons, including primers, are depicted. (Bottom) Diagram of the expected disruption after excision of exon 7 by the action of the Cre recombinase.

(B) Image of the electrophoretic migration in an agarose gel of the amplicons obtained using the indicated primers. Plus, plus-RT reaction; minus, minus-RT controls.

(C) Fluorescence image of an Alexa 594-filled Purkinje cell in a cerebellar slice from a *TRPC3*$^{-/-}$ mouse.

(D) (Left) Blockade of PF-evoked fast EPSC in a TRPC3-deficient mouse by CNQX (40 µM). (Right) Summary graph of EPSC blockade by CNQX (n = 5).

(E) (Top) Paired PF EPSCs evoked (interval of 100 ms) in a WT and in a *TRPC3*$^{-/-}$ mouse. (Bottom) Time course of facilitation in WT (n = 8 cells) and in *TRPC3*$^{-/-}$ (n = 11 cells) mice.

(F) Footprint patterns in WT and *TRPC3*$^{-/-}$ mice. The images show mice walking on a glass plate. Dotted lines depict their transverse body diameter. The right part of the panel summarizes the superimposed paw positions for 24 steps of 8 WT and *TRPC3*$^{-/-}$ mice.

in the lower scheme of Figure 3A. The expected disruption of the *TRPC3* gene was verified by gel electrophoresis of RT-PCR-products (Figure 3B) obtained using the primers indicated in Figure 3A.

The resulting TRPC3 knockout mice are viable, fertile, and appear normal with regard to their general appearance. Neither the size nor the layering structure of the cerebellum nor the morphology of Purkinje cells (Figure 3C) are affected by the absence of TRPC3. Fast synaptic transmission at PF synapses in response to single-shock stimulation in the TRPC3 knockouts is, as in the WT, completely blocked by CNQX (Figure 3D, n = 5 cells), indicating the exclusive role of AMPA receptors for fast synaptic excitation (Konnerth et al., 1990). AMPA receptor-mediated EPSCs had similar monoexponential decay time courses in *TRPC3*$^{-/-}$ (12.9 ± 0.9 ms, n = 11 cells) and in WT mice (11.6 ± 0.7 ms, n = 8 cells; p = 0.31). Paired-pulse facilitation that is a characteristic feature of PF-Purkinje cell synapses (Konnerth et al., 1990) is not altered in the TRPC3 knockout mice (Figure 3E, n = 11 cells in *TRPC3*$^{-/-}$ and 8 cells in WT mice). Thus, presynaptic glutamate release at this synapse is not affected by the inactivation of the *TRPC3* gene.

In contrast to *TRPC1*$^{-/-}$ mice (Figure S2), *TRPC3*$^{-/-}$ mice exhibited a distinct behavioral defect. Figure 3F shows a foot print analysis from representative WT and *TRPC3*$^{-/-}$ mice, respectively. In WT mice, the foot prints of both the front (black dots in Figure 3F) and the hindpaws (red symbols) were almost exclusively confined to a path of a width corresponding to the transverse body diameter. By contrast, in *TRPC3*$^{-/-}$ mice the foot prints of the hindpaws were mostly outside this path (Figure 3F, lower panel) as a result of a deficit in coordination. Similar observations were made in all mice tested (eight of each genotype). These results are summarized in the graph shown in Figure 3G. The movement deficit of the hindpaws was investigated in two additional tests involving walking on an irregularly spaced ladder (Figure 3H), as well as walking on a thin elevated beam (Figure 3I). In all these tests, *TRPC3*$^{-/-}$ mice performed much poorer than WT control mice.

In *TRPC3*$^{-/-}$ mice, the mGluR1-mediated slow EPSC at PF-Purkinje cell synapses (Figure 4A) was completely abolished in all 14 cells tested (Figures 4B and 4C). Remarkably, however, the synaptically evoked dendritic Ca^{2+} signal was virtually unaffected (Figures 4A–4C). Control experiments in which we used the mGluR1 antagonist CPCCOEt (Figure 4D) and cyclopiazonic acid (CPA) (Figure 4E), a drug that blocks the ATP-dependent uptake of Ca^{2+} ions into intracellular stores and therefore leads to their depletion (Ehrlich et al., 1994), confirmed that the Ca^{2+} transient recorded in *TRPC3*$^{-/-}$ mice is, as in WT, an mGluR1-evoked Ca^{2+} release signal from internal stores. Consistent with these findings, the DHPG-evoked slow inward current, but

(G) Percentage of hindpaw positions outside of the body diameter in both genotypes (summary of the results shown in (F).

(H) Percentage of hindpaw slips relative to the total number of steps on a horizontal ladder with an irregular spacing (n = 9 WT and 12 *TRPC3*$^{-/-}$ mice).

(I) Similar analysis of hindpaw slips during runs on an elevated beam (Ø = 1 cm; n = 8 WT and n = 10 *TRPC3*$^{-/-}$ mice).

Asterisks in (G)–(I) indicate high significance ($p < 0.01$, χ^2 test [G], Mann-Whitney U test [H and I]). Error bars indicate SEM.

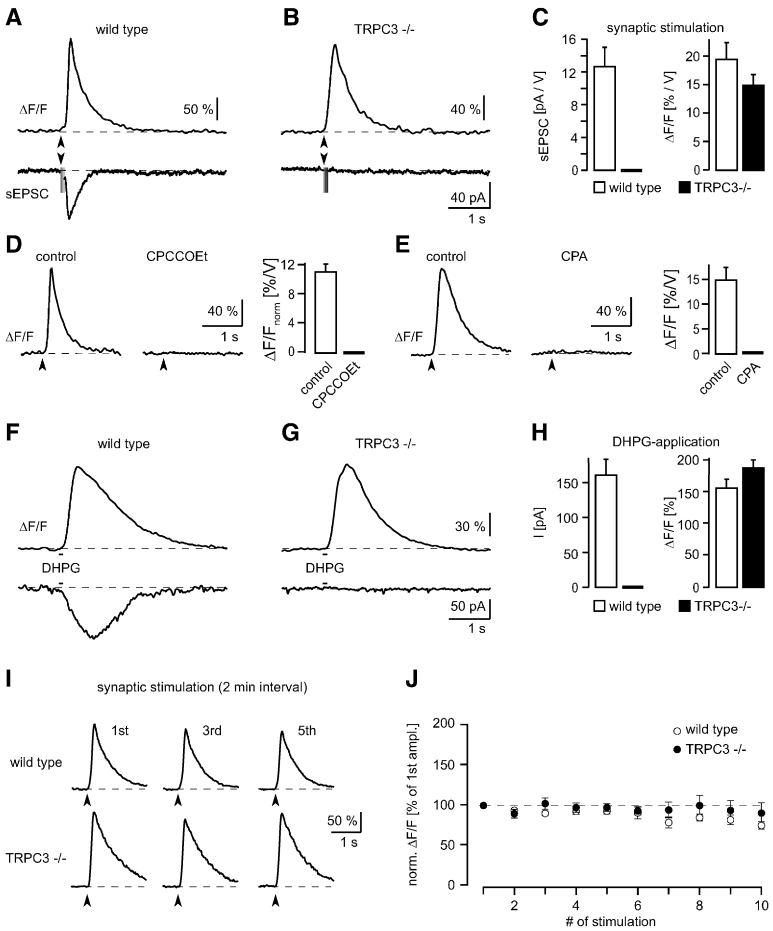

Figure 4. mGluR-Mediated Purkinje Cell Signaling in the Absence of TRPC3

(A) Slow EPSC in a WT mouse (lower trace) and the corresponding local dendritic Ca^{2+} response (upper trace).

(B) Similar recording in a *TRPC3*$^{-/-}$ mouse.

(C) Summary graphs for normalized (to stimulation strength) sEPCS (n = 41 in WT and n = 25 in *TRPC3*$^{-/-}$ mice) and Ca^{2+} transients (ΔF/F, n = 15 in WT and n = 17 in *TRPC3*$^{-/-}$ mice).

(D and E) Synaptically evoked local dendritic Ca^{2+} transients in *TRPC3*$^{-/-}$ mice before (control) and after the addition of CPCCOEt (D) and CPA (E). Bar graphs: Summary of the results (n = 4 cells for CPCCOEt and 6 cells for CPA).

(F) DHPG evoked a slow inward current (lower trace) and local Ca^{2+} transient (upper trace) in a WT mouse.

(G) Similar recording in a *TRPC3*$^{-/-}$ mouse.

(H) Summary of DHPG-evoked current (right) and Ca^{2+} (left) responses (n = 26 in WT and n = 30 in *TRPC3*$^{-/-}$ mice).

(I) Dendritic Ca^{2+} transients evoked by synaptic simulation in the two genotypes as indicated.

(J) Mean amplitudes of Ca^{2+} transients normalized to the first amplitude for ten subsequent stimuli in WT (n = 4 cells) and in *TRPC3*$^{-/-}$ mice (n = 6 cells). Error bars indicate SEM.

not the Ca^{2+} signal, were absent in *TRPC3*$^{-/-}$ mice (Figures 4F–4H). Finally, we tested the hypothesis (Kim et al., 2003) that the TRPC-mediated Ca^{2+} influx associated with the slow EPSC is needed for the replenishment of internal stores depleted by activation of the PLC-$InsP_3$ signaling cascade. For this purpose, we evoked at PF-Purkinje cell synapses repeatedly, at intervals of 2 min, mGluR1-mediated responses both in WT and *TRPC3*$^{-/-}$ mice (Figure 4I). We found that the amplitude of the mGluR1-mediated Ca^{2+} transients was robust during multiple stimulations (Figure 4J), indicating that TRPC3 has no decisive role for store replenishment.

DISCUSSION

In conclusion, we provide evidence that TRPC3 is required for both normal motor behavior and normal synaptic function in cerebellar Purkinje cells. In particular, we have shown that *TRPC3*$^{-/-}$ mice express a distinct defect concerning the normal functioning of the hindpaws during different walking tests (Figure 3). This behavioral phenotype is not as severe as the ataxic phenotypes encountered in mGluR-deficient (Aiba et al., 1994) or $G\alpha_q$-deficient mice (Hartmann et al., 2004; Offermanns et al., 1997), in which both the synaptically mediated Ca^{2+} release signal and the slow EPSC are absent. Instead, it is quite similar to the deficit in cerebellar motor control that we had observed previously in mice lacking calbindin D28k exclusively in Purkinje cells (Barski et al., 2003). The previously reported particularly high expression levels of TRPC3 in the cerebellum (Riccio et al., 2002) suggest that the behavioral deficit encountered in *TRPC3*$^{-/-}$ mice is largely due to an impaired cerebellar function.

We find that in *TRPC3*$^{-/-}$ mice the slow EPSC is totally absent while in mice lacking TRPC1 the slow EPSC is unaffected. This lack of evidence for an involvement of TRPC1 (Kim et al., 2003) in the generation of mGluR1-mediated slow EPSCs in adult mice is unexpected. Interestingly, in contrast to the general developmental pattern of TRP channels in the brain with a strong expression around birth followed by a downregulation at later stages (Li et al., 1999), TRPC3 in Purkinje cells is upregulated during development, reaching its maximum in adulthood (Huang et al., 2007). It is, therefore, possible that TRPC1 contributes to mGluR1-mediated signaling at early postnatal stages, when TRPC1 and TRPC3 are similarly abundantly expressed in Purkinje cells (Huang et al., 2007). Alternatively, the different results obtained by Kim et al. (2003) might also be explained by the fact that for their analysis they mostly used cultured slices, while we used exclusively acute slice preparations.

Besides the new role in synaptic transmission, there is evidence for specific roles of TRPC channels in early brain development. Thus, Li et al. (1999) reported that in most brain areas the expression of TRPC3 protein is particularly high during a narrow developmental time window before and after birth, suggesting an involvement of TRPC3 for the developmental formation of neuronal circuits. In line with this expression peak during early postnatal stages, it was found that TRPC3 channels are activated by brain-derived neurotrophic factor (BDNF) in cultured pontine neurons from neonatal rat brain (Li et al., 1999) and in cultured hippocampal CA1 pyramidal cells (Amaral and

Pozzo-Miller, 2007). The BDNF-activated TRPC3 conductance has been implicated in dendritic remodelling (Amaral and Pozzo-Miller, 2007). In further support of this view, it has been found that knockdown of TRPC3 expression with siRNAs inhibits BDNF-induced turning of growth cones in cultured cerebellar granule cells (Li et al., 2005).

The signaling cascade linking mGluR1 and TRPC3 requires the activation of G proteins of the $G\alpha_q$ type, as indicated by the total absence of the slow EPSC in $G\alpha_q$-deficient mice, which were analyzed under conditions that were similar to those used here (Hartmann et al., 2004). In addition, recordings performed in Purkinje cells from PLCβ4-deficient mice indicate that activation of the mGluR1-activated inward current requires PLCβ (Sugiyama et al., 1999; but see Canepari and Ogden, 2006). Further elements of the signaling pathway in in vivo Purkinje cells remain to be elucidated. It is noteworthy that despite the high Ca^{2+} permeability of TRPC3 channels (Kamouchi et al., 1999), mGluR1-activated Ca^{2+} entry contributes 2- to 4-fold less than the Ca^{2+} release from internal stores to the overall Ca^{2+} signal (Canepari and Ogden, 2006; J.H., H.A.H., and A.K., unpublished data). Consistent with this result, the synaptically evoked Ca^{2+} transient is strongly attenuated when blocking $InsP_3$ receptors or when emptying internal stores (Finch and Augustine, 1998; Takechi et al., 1998). In fact, earlier findings clearly show that the slow EPSC involves a marked influx of Na^+ ions (Knöpfel et al., 2000; Linden et al., 1994; Staub et al., 1992). Finally, it is remarkable that Ca^{2+} release from internal stores persists in the absence of TRPC1, TRPC4, TRPC6 (Figure 1), and even in the total absence of the mGluR1-activated inward current in *TRPC3*$^{-/-}$ mice (Figure 4). These findings indicate that in central neurons Ca^{2+} entry through TRPC channels is not required for refilling of the internal Ca^{2+} stores. Taken together, our results provide strong evidence that TRPC3 cation channels mediate slow synaptic excitation in cerebellar Purkinje cells and, thus, identify a key mechanism underlying slow synaptic excitation in the adult mammalian nervous system.

EXPERIMENTAL PROCEDURES

Generation of Mutant Mice

TRPC1/TRPC4 double-knockout (TRPC1/4 DKO) mice were generated by breeding *TRPC1*$^{-/-}$ (Dietrich et al., 2007) and *TRPC4*$^{-/-}$ mice (Freichel et al., 2001). By crossing *TRPC6*$^{-/-}$ mice (Dietrich et al., 2005) and TRPC1/4 DKO mice, we obtained TRPC1/TRPC4/TRPC6 triple-knockout (TRPC1/4/6 TKO) mice. *TRPC3*$^{-/-}$ mice were generated by disrupting the *TRPC3* gene in a three-step process as illustrated in Figure S2 (for details see Supplemental Data). For the behavioral tests, we used mice aged from postnatal day (P) 34 to P51. The mean age of mice used for the other experiments was P107 ± 79 (SD, n = 53).

Preparation of Tissue Slices

Mice were decapitated following anesthesia, and the cerebella were rapidly removed and placed in artificial cerebrospinal fluid (ACSF) (0°C–2°C) containing (in mM) 125 NaCl, 4.5 KCl, 2 $CaCl_2$, 1 $MgCl_2$, 1.25 NaH_2PO_4, 26 $NaHCO_3$, and 20 glucose, bubbled with 95% O_2 and 5% CO_2. Slices were cut using a vibratome slicer (Leica, Germany). After cutting, slices were kept for 1 hr at 34°C and then for up to 8 hr at room temperature in ACSF.

Immunohistochemistry

Acute slices (200 μM thick) were treated for immunodetection according to standard procedures (4% PFA, 0.3% Triton X-100, 5% goat serum). Anti-calbindin (mouse monoclonal 1:500, Swant, Switzerland) and anti-TRPC3 (rabbit polyclonal 1:100, Alomone, Israel) primary antibodies were incubated over night at 4°C. Alexa 488- (goat anti mouse 1:1000) and Alexa 555-labeled (goat anti-rabbit 1:1000, Invitrogen) secondary antibodies were incubated 2 hr at room temperature. Confocal images (LSM510, Zeiss, Germany) were maximum-intensity projected to visualize the immunoreactivity.

Electrophysiology

Whole-cell recordings were performed following standard procedures (Edwards et al., 1989). Patch pipettes (3–4 MΩ) were pulled from borosilicate glass (Hilgenberg, Germany) and coated with silicon (RTV 615, GE Silicons). The internal solution contained (in mM) 148 potassium gluconate, 10 HEPES, 10 NaCl, 0.5 $MgCl_2$, 4 Mg-ATP, 0.4 Na_3-GTP, and 0.1 Oregon Green BAPTA-1 (Molecular Probes, USA), pH 7.3. During the recordings, the slices were continuously perfused at room temperature with ACSF that contained 10 μM bicuculline (Sigma, Germany). Afferent stimulation was performed by using a patch pipette filled with 1 M NaCl (1 MΩ resistance).

Quantitative Rapid-Cycle Real-Time RT-PCR

Individual Purkinje cells and control material were harvested under visual control from cerebellar slices. Rapid-cycle PCR reactions were performed as previously described (Durand et al., 2006) (for details see Supplemental Data).

Statistical Analysis

All values are reported as means ± SEM. Statistical significance was tested using the Student's t test if not stated otherwise. The criterion for significance was $p < 0.05$.

SUPPLEMENTAL DATA

The Supplemental Data include Supplemental Experimental Procedures, figures, and a table and can be found with this article online at http://www.neuron.org/cgi/content/full/59/3/392/DC1/.

ACKNOWLEDGMENTS

Supported by the Deutsche Forschungsgemeinschaft (HA 5388/1-1; IRTG 1373, GRK 333), the Intramural Research Program of the NIH, National Institute of Environmental Health Sciences (Z01-ES101684), and the Schiedel Foundation. A.K. is a Carl-von-Linde Senior Fellow of the Institute for Advanced Study of the TUM.

Accepted: June 6, 2008
Published: August 13, 2008

REFERENCES

Aiba, A., Kano, M., Chen, C., Stanton, M.E., Fox, G.D., Herrup, K., Zwingman, T.A., and Tonegawa, S. (1994). Deficient cerebellar long-term depression and impaired motor learning in mGluR1 mutant mice. Cell *79*, 377–388.

Amaral, M.D., and Pozzo-Miller, L. (2007). TRPC3 channels are necessary for brain-derived neurotrophic factor to activate a nonselective cationic current and to induce dendritic spine formation. J. Neurosci. *27*, 5179–5189.

Barski, J.J., Hartmann, J., Rose, C.R., Hoebeek, F., Mörl, K., Noll-Hussong, M., De Zeeuw, C.I., Konnerth, A., and Meyer, M. (2003). Calbindin in cerebellar Purkinje cells is a critical determinant of the precision of motor coordination. J. Neurosci. *23*, 3469–3477.

Batchelor, A.M., and Garthwaite, J. (1993). Novel synaptic potentials in cerebellar Purkinje cells: probable mediation by metabotropic glutamate receptors. Neuropharmacology *32*, 11–20.

Canepari, M., and Ogden, D. (2006). Kinetic, pharmacological and activity-dependent separation of two Ca^{2+} signalling pathways mediated by type 1 metabotropic glutamate receptors in rat Purkinje neurones. J. Physiol. *573*, 65–82.

Canepari, M., Papageorgiou, G., Corrie, J.E., Watkins, C., and Ogden, D. (2001). The conductance underlying the parallel fibre slow EPSP in rat cerebellar Purkinje neurones studied with photolytic release of L-glutamate. J. Physiol. *533*, 765–772.

Dietrich, A., Mederos, Y.S.M., Gollasch, M., Gross, V., Storch, U., Dubrovska, G., Obst, M., Yildirim, E., Salanova, B., Kalwa, H., et al. (2005). Increased vascular smooth muscle contractility in TRPC6−/− mice. Mol. Cell. Biol. *25*, 6980–6989.

Dietrich, A., Kalwa, H., Storch, U., Mederos, Y.S.M., Salanova, B., Pinkenburg, O., Dubrovska, G., Essin, K., Gollasch, M., Birnbaumer, L., and Gudermann, T. (2007). Pressure-induced and store-operated cation influx in vascular smooth muscle cells is independent of TRPC1. Pflugers Arch. *455*, 465–477.

Durand, G.M., Marandi, N., Herberger, S.D., Blum, R., and Konnerth, A. (2006). Quantitative single-cell RT-PCR and Ca^{2+} imaging in brain slices. Pflugers Arch. *451*, 716–726.

Edwards, F.A., Konnerth, A., Sakmann, B., and Takahashi, T. (1989). A thin slice preparation for patch clamp recordings from neurones of the mammalian central nervous system. Pflugers Arch. *414*, 600–612.

Ehrlich, B.E., Kaftan, E., Bezprozvannaya, S., and Bezprozvanny, I. (1994). The pharmacology of intracellular Ca^{2+}-release channels. Trends Pharmacol. Sci. *15*, 145–149.

Eilers, J., Augustine, G.J., and Konnerth, A. (1995). Subthreshold synaptic Ca^{2+} signalling in fine dendrites and spines of cerebellar Purkinje neurons. Nature *373*, 155–158.

Finch, E.A., and Augustine, G.J. (1998). Local calcium signalling by inositol-1,4,5-trisphosphate in Purkinje cell dendrites. Nature *396*, 753–756.

Freichel, M., Suh, S.H., Pfeifer, A., Schweig, U., Trost, C., Weissgerber, P., Biel, M., Philipp, S., Freise, D., Droogmans, G., et al. (2001). Lack of an endothelial store-operated Ca^{2+} current impairs agonist-dependent vasorelaxation in TRP4−/− mice. Nat. Cell Biol. *3*, 121–127.

Hartmann, J., Blum, R., Kovalchuk, Y., Adelsberger, H., Kuner, R., Durand, G.M., Miyata, M., Kano, M., Offermanns, S., and Konnerth, A. (2004). Distinct roles of $G\alpha_q$ and $G\alpha_{11}$ for Purkinje cell signaling and motor behavior. J. Neurosci. *24*, 5119–5130.

Hirono, M., Konishi, S., and Yoshioka, T. (1998). Phospholipase C-independent group I metabotropic glutamate receptor- mediated inward current in mouse Purkinje cells. Biochem. Biophys. Res. Commun. *251*, 753–758.

Huang, W.C., Young, J.S., and Glitsch, M.D. (2007). Changes in TRPC channel expression during postnatal development of cerebellar neurons. Cell Calcium *42*, 1–10.

Ichise, T., Kano, M., Hashimoto, K., Yanagihara, D., Nakao, K., Shigemoto, R., Katsuki, M., and Aiba, A. (2000). mGluR1 in cerebellar Purkinje cells essential for long-term depression, synapse elimination, and motor coordination. Science *288*, 1832–1835.

Kamouchi, M., Philipp, S., Flockerzi, V., Wissenbach, U., Mamin, A., Raeymaekers, L., Eggermont, J., Droogmans, G., and Nilius, B. (1999). Properties of heterologously expressed hTRP3 channels in bovine pulmonary artery endothelial cells. J. Physiol. *518*, 345–358.

Kim, S.J., Kim, Y.S., Yuan, J.P., Petralia, R.S., Worley, P.F., and Linden, D.J. (2003). Activation of the TRPC1 cation channel by metabotropic glutamate receptor mGluR1. Nature *426*, 285–291.

Knöpfel, T., Anchisi, D., Alojado, M.E., Tempia, F., and Strata, P. (2000). Elevation of intradendritic sodium concentration mediated by synaptic activation of metabotropic glutamate receptors in cerebellar Purkinje cells. Eur. J. Neurosci. *12*, 2199–2204.

Konnerth, A., Llano, I., and Armstrong, C.M. (1990). Synaptic currents in cerebellar Purkinje cells. Proc. Natl. Acad. Sci. USA *87*, 2662–2665.

Li, H.S., Xu, X.Z., and Montell, C. (1999). Activation of a TRPC3-dependent cation current through the neurotrophin BDNF. Neuron *24*, 261–273.

Li, Y., Jia, Y.C., Cui, K., Li, N., Zheng, Z.Y., Wang, Y.Z., and Yuan, X.B. (2005). Essential role of TRPC channels in the guidance of nerve growth cones by brain-derived neurotrophic factor. Nature *434*, 894–898.

Liman, E.R., Corey, D.P., and Dulac, C. (1999). TRP2: a candidate transduction channel for mammalian pheromone sensory signaling. Proc. Natl. Acad. Sci. USA *96*, 5791–5796.

Linden, D.J., Smeyne, M., and Connor, J.A. (1994). Trans-ACPD, a metabotropic receptor agonist, produces calcium mobilization and an inward current in cultured cerebellar Purkinje neurons. J. Neurophysiol. *71*, 1992–1998.

Martin, L.J., Blackstone, C.D., Huganir, R.L., and Price, D.L. (1992). Cellular localization of a metabotropic glutamate receptor in rat brain. Neuron *9*, 259–270.

Offermanns, S., Hashimoto, K., Watanabe, M., Sun, W., Kurihara, H., Thompson, R.F., Inoue, Y., Kano, M., and Simon, M.I. (1997). Impaired motor coordination and persistent multiple climbing fiber innervation of cerebellar Purkinje cells in mice lacking $G\alpha_q$. Proc. Natl. Acad. Sci. USA *94*, 14089–14094.

Ramsey, I.S., Delling, M., and Clapham, D.E. (2006). An introduction to TRP channels. Annu. Rev. Physiol. *68*, 619–647.

Riccio, A., Medhurst, A.D., Mattei, C., Kelsell, R.E., Calver, A.R., Randall, A.D., Benham, C.D., and Pangalos, M.N. (2002). mRNA distribution analysis of human TRPC family in CNS and peripheral tissues. Brain Res. Mol. Brain Res. *109*, 95–104.

Staub, C., Vranesic, I., and Knöpfel, T. (1992). Responses to metabotropic glutamate receptor activation in cerebellar Purkinje cells: induction of an inward current. Eur. J. Neurosci. *4*, 832–839.

Sugiyama, H., Ito, I., and Hirono, C. (1987). A new type of glutamate receptor linked to inositol phospholipid metabolism. Nature *325*, 531–533.

Sugiyama, T., Hirono, M., Suzuki, K., Nakamura, Y., Aiba, A., Nakamura, K., Nakao, K., Katsuki, M., and Yoshioka, T. (1999). Localization of phospholipase Cβ isozymes in the mouse cerebellum. Biochem. Biophys. Res. Commun. *265*, 473–478.

Takechi, H., Eilers, J., and Konnerth, A. (1998). A new class of synaptic response involving calcium release in dendritic spines. Nature *396*, 757–760.

Tallquist, M.D., and Soriano, P. (2000). Epiblast-restricted Cre expression in MORE mice: a tool to distinguish embryonic vs. extra-embryonic gene function. Genesis *26*, 113–115.

Tempia, F., Alojado, M.E., Strata, P., and Knöpfel, T. (2001). Characterization of the mGluR(1)-mediated electrical and calcium signaling in Purkinje cells of mouse cerebellar slices. J. Neurophysiol. *86*, 1389–1397.

Venkatachalam, K., and Montell, C. (2007). TRP channels. Annu. Rev. Biochem. *76*, 387–417.